5.A. SYNTHESIS OF ACETONAPHTHONES TETHERED PIPERIDINE-3-CARBOXYLIC ACID DERIVATIVES [SERIES 1]

5.A.1. CHEMISTRY

Compounds **(3S1a-3S1i)** were synthesised in two steps and compounds **(4S1a -4S1i)** in 3 steps as per the reaction sequence outlined in **Scheme 4.1**. The intermediates i.e. respective bromomethyl naphthyl ketones were synthesized by the selective bromination of corresponding α-naphthyl ketones with a suspension of copper (II) bromide in chloroform-ethylacetate (1:1) [King and Ostrum, 1964]. The title compounds were prepared by the N-alkylation of piperidine-3-carboxylic acid ethyl ester with the appropriate bromomethyl naphthyl ketone. The bromomethyl naphthyl ketones were stirred with ethyl nepicotate and potassium carbonate in THF initially for two hours in an ice bath and then for 30 h at room temperature to obtain the target compounds **(3S1a-3S1i)**. The ester derivative of the parent cyclic amino acid, i.e., ethyl nipecotate was used for the synthesis of derivatives **(3S1a-3S1i)** to protect the carboxyl group in this reaction. The ethyl ester group of N-alkylated derivatives was finally hydrolyzed in ethanol under basic condition (NaOH) to yield the free N-substituted piperidine-3-carboxylic acid **(4S1a-4S1i) (Table 5.1)**.

5.A.1.1. Physicochemical Characterization

The solvent system used to determine the R_f values and monitor the progress of reaction was n-hexane/ethyl acetate (6:4). Subsequently, the percentage yield of the title compounds was calculated. The Log P value of synthesised compounds was determined by octanol/water "shake-flask" method to establish lipophilicity. The general chemical structure and the physicochemical properties of the final compounds **(3S1a-3S1i & 4S1a-4S1i)** are presented in **Table 5.1**.

Table 5.1. Chemical Structures and Physicochemical Properties of Compounds **(3S1a-3S1i & 4S1a-4S1i)**

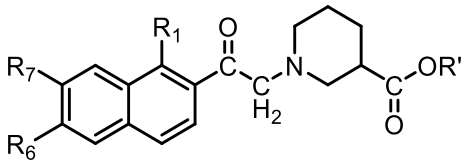

Comp.	R'	R_1	R_6	R_7	R_f[a]	Log P[b]
3S1a	C_2H_5	H	H	H	0.43	2.56
3S1b	C_2H_5	H	CH3	H	0.42	2.94
3S1c	C_2H_5	H	OCH_3	H	0.41	2.71
3S1d	C_2H_5	H	Cl	H	0.34	3.18
3S1e	C_2H_5	H	Br	H	0.32	3.50
3S1f	C_2H_5	H	CH_3	CH_3	0.48	3.58
3S1g	C_2H_5	OCH_3	H	H	0.49	2.49
3S1h	C_2H_5	H	OCH_3	OCH_3	0.51	2.64
3S1i	C_2H_5	H	C_2H_5	H	0.42	3.82
4S1a	H	H	H	H	0.53	2.38
4S1b	H	H	CH3	H	0.56	2.80
4S1c	H	H	OCH_3	H	0.58	2.30
4S1d	H	H	Cl	H	0.39	2.97
4S1e	H	H	Br	H	0.37	3.35
4S1f	H	H	CH_3	CH_3	0.58	3.39
4S1g	H	OCH_3	H	H	0.45	2.20
4S1h	H	H	OCH_3	OCH_3	0.57	2.12
4S1i	H	H	C_2H_5	H	0.44	3.47

R_f values are determined using hexane/EtOAc (6:4) as mobile phase.
[b]Log P values of all the compounds were determined experimentally using shake flask method.

5.A.1.2. Spectral Characterization and Elemental Analysis

The structures of compounds were characterised by FT–IR, ^{1}H NMR, ^{13}C NMR and elemental (C, H, N) analysis. The FT-IR spectra of the compounds **(3S1a-3S1i and 4S1a-4S1i)** exhibited the characteristic medium C=O stretching of naphthyl ketone in the range of 1690-1790 cm^{-1}.

The ^{1}H–NMR of compounds **4S1a-4S1i** showed a peak of the acid at down field (11.80-10.00 ppm), while compounds **3S1a-3S1i** showed a triplet peak of three protons of methyl (–CH_3) at 1.31-1.10 ppm and the quartet peak of CH_2 protons at 4.30-4.20 ppm. The protons of methylene bridge (–CH_2) were observed as singlet in the range of 3.83–3.50 ppm. The ^{1}H–NMR of all the compounds exhibited the aromatic protons of naphthalene in the range of 7.10–8.80 ppm and aliphatic proton of nipecotic acid in the range of 3.60–1.20 ppm. ^{13}C-NMR spectra also supported the ^{1}H–NMR mentioned above. In ^{13}C-NMR spectra, the presence of carboxylate group for compounds **4S1a-4S1i** was confirmed by a peak near to 200 δ at down field. All other ^{13}C NMR peaks were seen as per the expected chemical shift. Results of the elemental analysis were within ± 0.4% of the theoretical values.

Ethyl 1-(2-(naphthalen-2-yl)-2-oxoethyl)piperidine-3-carboxylate (3S1a)

Yield: 342 mg, 52.4% as colorless oil. FT-IR (KBr, cm^{-1}): 3124 (Ar-H Str.), 2941 (C-H Str.), 1735 (C=O Str.), 1307 (C-N Str.), 1242 (C-O Str.), 1051 (C-O Str.). ^{1}H NMR (500 MHz, $CDCl_3$) δ ppm: 8.50 (m, 2H, naphthalene), 8.0-8.20 (t, *J* = 6.5 Hz, 2H naphthalene), 7.80 (d, *J* = 8.5Hz, 1H, naphthalene), 7.60 (t, *J* = 7.5 Hz, 2H, naphthalene), 4.21 (q, *J* = 5.8 Hz, 2H, CH_2 carboxylate), 3.88 (s, 1H, NCH_2), 3.78 (s, 1H, NCH_2), 2.45-2.30 (m, 5H, piperidine), 1.70-1.50 (m, 4H, piperidine), 1.21 (t, *J* = 6.0 Hz, 3H, CH_3 carboxylate). ^{13}C NMR (125 MHz, $CDCl_3$) δ ppm: 194.3, 174.4, 135.1, 133.1, 130.1, 129.8, 127.9, 126.8, 125.7, 71.7, 63.2, 57.4, 47.3, 25.2, 22.8, 14.7. Anal. calc. for **$C_{20}H_{23}NO_3$**: C, 73.82; H, 7.12; N, 4.30; Found: C, 73.75; H, 7.10; N, 4.31.

Ethyl 1-(2-(6-methylnaphthalen-2-yl)-2-oxoethyl)piperidine-3-carboxylate (3S1b)

Yield: 268 mg, 39.6% as colorless oil. FT-IR (KBr, cm^{-1}): 3078 (Ar-H Str.), 2821 (C-H Str.), 1738 (C=O Str.), 1298 (C-N Str.), 1245 (C-O Str.), 1047 (C-O Str.). ^{1}H NMR (500 MHz, $CDCl_3$) δ ppm: 8.40 (s, 1H, naphthalene), 8.10 (s, 1H, naphthalene), 7.80-

7.70 (dd, *J* = 5.0 Hz, 2H naphthalene), 7.50 (m, 2H, naphthalene), 4.30 (q, *J* = 6.0 Hz, 2H, CH_2 carboxylate), 3.68 (s, 1H, NCH_2), 3.58 (s, 1H, NCH_2), 2.65-2.30 (m, 5H, piperidine), 2.60 (s, 3H, CH_3, naphthalene), 1.70-1.50 (m, 4H, piperidine), 1.31 (t, *J* = 6.2 Hz, 3H, CH_3 carboxylate). ^{13}C NMR (125 MHz, $CDCl_3$) δ ppm: 196.8, 171.0, 138.1, 135.1, 133.1, 130.1, 129.8, 127.9, 126.8, 125.7, 72.3, 63.1, 57.8, 47.4, 25.7, 21.4, 22.5, 15.3. Anal. calc. for **$C_{21}H_{25}NO_3$:** C, 74.31; H, 7.42; N, 4.13; Found: C, 74.45; H, 7.44; N, 4.12.

Ethyl 1-(2-(6-methoxynaphthalen-2-yl)-2-oxoethyl)piperidine-3 carboxylate (3S1c)

Yield: 321 mg, 45.2% as light yellow oil. FT-IR (KBr, cm^{-1}): 3087(Ar-H Str.), 2864 (C-H Str.), 1790 (C=O Str.), 1304 (C-N Str.), 1245 (C-O Str.), 1043 (C-O Str.). ^{1}H NMR (500 MHz, $CDCl_3$) δ ppm: 8.45 (s, 1H, naphthalene, C_1,), 8.20 (s, 1H, naphthalene), 7.80-7.65 (dd, *J* = 5.5 Hz, 2H naphthalene), 7.30 (s, *J* = 6.0 Hz, 1H, naphthalene), 7.20 (d, *J* = 5.5 Hz, 1H, naphthalene), 4.20 (q, *J* = 6.2 Hz, 2H, CH_2 carboxylate), 3.80 (s, 1H, NCH_2), 3.71 (s, 1H, NCH_2), 2.75-2.30 (m, 5H, piperidine), 1.90-1.50 (m, 4H, piperidine), 1.26 (t, *J* = 5.8 Hz, 3H, CH_3 carboxylate). ^{13}C NMR (125 MHz, $CDCl_3$) δ ppm: 191.4, 174.5, 161.3, 138.1, 135.1, 133.1, 130.1, 129.8, 127.9, 126.8, 125.7, 106.1, 71.3, 63.1, 59.2, 58.3, 46.3, 28.2, 24.7, 14.5. Anal. calc. for **$C_{21}H_{25}NO_4$:** C, 70.96; H, 7.09; N, 3.94; Found: C, 70.81; H, 7.07; N, 3.95.

Ethyl 1-(2-(6-chloronaphthalen-2-yl)-2-oxoethyl)piperidine-3-carboxylate (3S1d)

Yield: 400 mg, 55.7% as brown yellow oil. FT-IR (KBr, cm^{-1}): 2974 (Ar-H Str.), 2675 (C-H Str.), 1784 (C=O Str.), 1329 (C-N Str.), 1251 (C-O Str.), 1057 (C-O Str.), 755 (C-Cl Str.). ^{1}H NMR (500 MHz, $CDCl_3$) δ ppm: 8.45 (s, 1H, naphthalene), 8.30 (s, 1H, naphthalene), 7.90 (s, 1H, naphthalene), 7.80 (d, *J* = 7.5 Hz, 1H, naphthalene), 7.60-7.55 (dd, *J* = 5.0 Hz, 2H, naphthalene), 4.28 (q, *J* = 5.8 Hz, 2H, CH_2 carboxylate), 3.70 (s, 1H, NCH_2), 3.69 (s, 1H, NCH_2), 2.80-2.30 (m, 5H, piperidine), 1.90-1.40 (m,

4H, piperidine), 1.24 (t, *J* = 6.0 Hz, 3H, CH_3 carboxylate). ^{13}C NMR (125 MHz, $CDCl_3$) δ ppm: 197.08, 173.95, 136.39, 135.52, 132.57, 131.55, 130.71, 129.19, 128.91, 127.12, 126.75, 64.06, 61.80, 55.86, 53.66, 44.72, 24.88, 22.66, 14.70. Anal. calc. for **$C_{20}H_{22}ClNO_3$:** C, 66.75; H, 6.16; N, 3.89; Found: C, 66.82, H, 6.18; N, 3.88.

Ethyl 1-(2-(6-bromonaphthalen-2-yl)-2-oxoethyl)piperidine-3-carboxylate (3S1e)

Yield: 402 mg, 49.8% as brown oil. FT-IR (KBr, cm^{-1}): 3089 (Ar-H Str.), 2879 (C-H Str.), 1738 (C=O Str.), 1325 (C-N Str.), 1255 (C-O Str.), 1054 (C-O Str.), 547 (C-Br Str.)**.** ^1H NMR (500 MHz, $CDCl_3$) δ ppm: 8.35 (s, 1H, naphthalene), 8.20 (s, 1H, naphthalene), 7.80 (s, 1H, naphthalene), 7.75 (d, *J* = 8.5 Hz, 1H, naphthalene), 7.61-7.52 (dd, *J* = 5.5 Hz, 2H naphthalene), 4.26 (q, *J* = 5.8 Hz, 2H, CH_2 carboxylate), 3.68 (s, 1H, NCH_2), 3.59 (s, 1H, NCH_2), 2.70-2.30 (m, 5H, piperidine), 1.90-1.45 (m, 4H, piperidine), 1.22 (t, *J* = 5.8 Hz, 3H, CH_3 carboxylate). ^{13}C NMR (125 MHz, $CDCl_3$) δ ppm: 197.08, 173.95, 141.03, 139.16, 137.22, 135.89, 133.97, 130.54, 130.34, 129.43, 126.61, 123.24, 64.06, 61.80, 55.86, 53.66, 44.72, 24.88, 22.66, 19.83, 14.70. Anal. calc. for **$C_{20}H_{22}BrNO_3$**: C, 59.42; H, 5.48; N, 3.46; Found: C, 59.27, H, 5.50; N, 3.47.

Ethyl 1-(2-(6,7-dimethylnaphthalen-2-yl)-2-oxoethyl)piperidine-3-carboxylate (3S1f)

Yield: 325 mg, 46.1% as colorless yellow oil. FT-IR (KBr, cm^{-1}): 3029 (Ar-H Str.), 2862 (C-H Str.), 1759 (C=O Str.), 1354 (C-N Str.), 1274 (C-O Str.), 1048 (C-O Str.)**.** ^1H NMR (500 MHz, $CDCl_3$) δ ppm: 8.30 (s, 1H, naphthalene), 8.10 (d, *J* = 8.5 Hz, 1H, naphthalene), 7.82 (d, *J* = 6.5 Hz, 1H, naphthalene), 7.50 (d, *J* = 5.5 Hz, 2H naphthalene), 4.30 (q, *J* = 6.2 Hz, 2H, CH_2 carboxylate), 3.66 (s, 1H, NCH_2), 3.55 (s, 1H, NCH_2), 3.50 (s, 6H, CH_3×2, naphthalene), 2.70-2.30 (m, 5H, piperidine), 1.70-1.40 (m, 4H, piperidine), 1.27 (t, *J* = 6.0 Hz, 3H, CH_3 carboxylate). ^{13}C NMR (125 MHz, $CDCl_3$) δ ppm: 197.08, 173.95, 141.03, 139.16, 137.22, 135.89, 133.97, 130.54, 130.34, 129.43, 126.61, 123.24, 64.06, 61.80, 55.86, 53.66, 45.72, 24.89, 22.86,

19.73, 14.74. Anal. calc. for **$C_{22}H_{27}NO_3$:** C, 74.76; H, 7.70; N, 3.96; Found: C, 74.52, H, 7.68; N, 3.96.

Ethyl 1-(2-(1-methoxynaphthalen-2-yl)-2-oxoethyl)piperidine-3-carboxylate (3S1g)

Yield: 361 mg, 50.9% as light yellow oil. FT-IR (KBr, cm^{-1}): 3058 (Ar-H Str.), 2732 (C-H Str.), 1765 (C=O Str.), 1347 (C-N Str.), 1253 (C-O Str.), 1058 (C-O Str.)**.** ^{1}H NMR (500 MHz, $CDCl_3$) δ ppm: 8.40 (d, *J* = 8.5 Hz, 1H, naphthalene), 8.10 (d, *J* = 6.5 Hz, 1H, naphthalene), 7.70-7.60 (m, 4H, naphthalene), 4.25 (q, *J* = 5.8 Hz, 2H, CH_2 carboxylate), 3.80 (s, 3H, OCH_3, naphthalene), 3.70 (s, 1H, NCH_2), 3.60 (s, 1H, NCH_2), 2.80-2.35 (m, 5H, piperidine), 1.65-1.40 (m, 4H, piperidine), 1.20 (t, *J* = 6.0 Hz, 3H, CH_3 carboxylate). ^{13}C NMR (125 MHz, $CDCl_3$) δ ppm: 196.10, 173.95, 156.32, 134.01, 129.57, 128.54, 126.76, 126.15, 124.77, 121.40, 63.38, 61.80, 60.86, 55.86, 53.66, 44.72, 24.88, 22.66), 14.70. Anal. calc. for **$C_{21}H_{25}NO_4$:** C, 70.96; H, 7.09; N, 3.94; Found: C, 70.92, H, 7.06; N, 3.95.

Ethyl 1-(2-(6,7-dimethoxynaphthalen-2-yl)-2-oxoethyl)piperidine-3-carboxylate (3S1h)

Yield: 432 mg, 56.1% as dark yellow oil. FT-IR (KBr, cm^{-1}): 2974 (Ar-H Str.), 2514 (C-H Str.), 1714 (C=O Str.), 1395 (C-N Str.), 1258 (C-O Str.), 1087 (C-O Str.)**.** ^{1}H NMR (500 MHz, $CDCl_3$) δ ppm: 8.42 (s, 1H, naphthalene, C_1,), 8.32 (d, *J* = 7.5 Hz, 1H, naphthalene), 7.45 (d, *J* = 7.5 Hz, 1H, naphthalene), 7.21 (d, *J* = 8.5 Hz, 2H naphthalene), 4.32 (q, *J* = 6.0 Hz, 2H, CH_2 carboxylate), 3.92 (s, 6H, 2×OCH_3, naphthalene), 3.72 (s, 1H, NCH_2), 3.61 (s, 1H, NCH_2),2.84-2.41 (m, 5H, piperidine), 1.80-1.30 (m, 4H, piperidine), 1.18 (t, *J* = 6.0 Hz, 3H, CH_3 carboxylate). ^{13}C NMR (125 MHz, $CDCl_3$) δ ppm: 197.08, 173.95, 152.07, 151.03, 137.32, 135.96, 133.23, 128.81, 127.08, 124.51, 109.01, 107.33, 64.06, 61.80, 56.58, 55.86, 51.66, 43.72,

24.84, 22.96, 13.70. Anal. calc. for **$C_{22}H_{27}NO_5$:** C, 68.55; H, 7.06; N, 3.63; Found: C, 68.76, H, 7.04; N, 3.64.

Ethyl 1-(2-(6-ethylnaphthalen-2-yl)-2-oxoethyl)piperidine-3-carboxylate (3S1i)

Yield: 393 mg, 55.7% as dark yellow oil. FT-IR (KBr, cm^{-1}): 2963 (Ar-H Str.), 2551 (C-H Str.), 1752 (C=O Str.), 1325 (C-N Str.), 1287 (C-O Str.), 1054 (C-O Str.)**.** ^{1}H NMR (500 MHz, $CDCl_3$) δ ppm: 8.50 (s, 1H, naphthalene), 8.15 (s, 1H, naphthalene), 7.85-7.70 (dd, 2H naphthalene), 7.50 (m, 2H, naphthalene), 4.20 (q, *J* = 5.8 Hz, 2H, CH_2 carboxylate), 3.73 (s, 1H, NCH_2), 3.64 (s, 1H, NCH_2), 2.60 (s, 2H, CH_2 naphthalene), 2.55-2.30 (m, 5H, piperidine), 1.9-1.4 (m, 4H, piperidine), 1.20 (s, 3H, CH_3 naphthalene), 1.11 (t, *J* = 6.0 Hz, 3H, CH_3 carboxylate). ^{13}C NMR (125 MHz, $CDCl_3$) δ ppm: 197.08, 173.95, 143.79, 138.12, 135.85, 131.37, 131.10, 128.75, 128.54, 127.41, 125.40, 64.06, 61.80, 55.86, 53.66, 44.65, 27.42, 24.87, 22.61, 14.85, 13.22. Anal. calc. for **$C_{22}H_{27}NO_3$:** C, 74.76; H, 7.70; N, 3.96; Found: C, 74.71, H, 7.68; N, 3.95.

1-(2-(Naphthalen-2-yl)-2-oxoethyl)piperidine-3-carboxylic acid (4S1a)

Yield: 173 mg, 58.4% as dark yellow oil. FT-IR (KBr, cm^{-1}): 3425 (OH Str.), 3083 (Ar-H Str.), 2853 (C-H Str.), 1719 (C=O Str.), 1260 (C-N Str.), 1142 (C-O Str.). ^{1}H NMR (500 MHz, $CDCl_3$) δ ppm: 11.12 (s 1H, COOH), 7.90 (s, 2H, naphthalene), 7.53 (dd, *J* = 5.0 Hz, 2H, naphthalene), 7.31 (d, *J* = 8.5 Hz, 1H naphthalene), 7.22-7.15 (m, 2H, naphthalene), 3.34 (s, 1H, NCH_2), 3.24 (s, 1H, NCH_2), 2.82-2.30 (m, 6H, piperidine), 1.38-1.34 (m, 3H, piperidine). ^{13}C NMR (125 MHz, $CDCl_3$) δ ppm: 197.3, 176.6, 138.6, 134.7, 134.2, 129.9, 128.8, 128.4, 127.2, 126.7, 124.7, 64.2, 55.6, 53.9, 41.2, 25.2, 22.9. Anal. calc. for **$C_{18}H_{19}NO_3$:** C, 72.71; H, 6.44; N, 4.71; Found: C, 72.58, H, 6.45; N, 4.70.

1-(2-(6-Methylnaphthalen-2-yl)-2-oxoethyl)piperidine-3-carboxylic acid (4S1b)

Yield: 156 mg, 50.3% as dark yellow oil. FT-IR (KBr, cm^{-1}): 3471 (OH Str.), 3034 (Ar-H Str.), 2961 (C-H Str.), 1728 (C=O Str.), 1282 (C-N Str.), 1085 (C-O Str). ^{1}H NMR (500 MHz, $CDCl_3$) 10.08 (s, 1H, COOH), 8.62 (d, *J* = 7.5 Hz, 2H, naphthalene), 8.19 (d, *J* = 9.0 Hz, 1H naphthalene), 8.02-7.94 (m, 3H, naphthalene), 4.12 (s, 2H, NCH_2), 4.02 (s, 2H, NCH_2), 3.60-2.84 (m, 6H, piperidine), 2.20-2.12 (m, 3H, piperidine). ^{13}C NMR (125 MHz, $CDCl_3$) δ ppm: 192.5, 171.8, 133.3, 130.7, 130.1, 128.8, 125.5, 125.0, 123.9, 123.3, 123.2, 121.0, 59.5, 50.8, 49.1, 36.4, 20.4, 18.1, 17.1. Anal. calc. for **$C_{19}H_{21}NO_3$**: C, 73.29; H, 6.80; N, 4.50; Found: C, 73.40, H, 6.78; N, 4.50.

1-(2-(6-Methoxynaphthalen-2-yl)-2-oxoethyl)piperidine-3-carboxylic acid (4S1c)

Yield: 197 mg, 60.2% as dark yellow oil. FT-IR (KBr, cm^{-1}): 3332 (OH Str.), 2988 (Ar-H Str.), 2964 (C-H Str.), 1690 (C=O Str.), 1345 (C-N Str.), 1145 (C-O Str.), 1043 (C-O Str.). ^{1}H NMR (500 MHz, $CDCl_3$) δ ppm: 11.32 (s, 1H, COOH), 8.40 (d, *J* = 6.5 Hz, 2H, naphthalene), 7.80-7.65 (dd, *J* = 5.0 Hz, 2H naphthalene), 7.30 (m, 2H, naphthalene), 3.80 (s, 1H, NCH_2), 3.70 (s, 1H, NCH_2), 3.60 (s, 3H, naphthalene, OCH_3,), 2.75-2.30 (m, 5H, piperidine), 1-93-1.56 (m, 4H, piperidine). ^{13}C NMR (125 MHz, $CDCl_3$) δ ppm: 196.3, 174.0, 161.3, 138.1, 135.1, 133.1, 130.1, 129.8, 127.9, 126.8, 125.7, 106.1, 71.3, 57.1, 56.3, 47.3, 24.9, 23.2. Anal. calc. for **$C_{19}H_{21}NO_4$:** C, 69.71; H, 6.47; N, 4.28; Found: C, 69.93, H, 6.47; N, 4.29.

1-(2-(6-Chloronaphthalen-2-yl)-2-oxoethyl)piperidine-3-carboxylic acid (4S1d)

Yield: 165 mg, 49.8% as dark yellow oil. FT-IR (KBr, cm^{-1}): 3436 (OH Str.), 2987 (Ar-H Str.), 2745 (C-H Str.), 1691 (C=O Str.), 1372 (C-N Str.), 1207 (C-O Str.) 645 (C-Cl Str.). ^{1}H NMR (500 MHz, $CDCl_3$) δ ppm: 10.94 (s, 1H, COOH), 8.45 (s, 2H, naphthalene), 7.90 (s, 1H, naphthalene), 7.80 (d, *J* = 7.5 Hz, 1H, naphthalene), 7.60-7.55 (dd, *J* = 5.0 Hz, 2H naphthalene), 3.60 (s, 1H, NCH_2), 3.50 (s, 1H, NCH_2), 2.70-

2.30 (m, 5H, piperidine), 1.74-1.48 (m, 4H, piperidine). ^{13}C NMR (125 MHz, $CDCl_3$) δ ppm: 196.3, 174.0, 161.3, 138.1, 135.1, 134.8, 133.1, 130.1, 129.8, 127.9, 126.8, 125.7, 71.3, 57.1, 47.3, 24.5, 23.4. Anal. calc. for **$C_{18}H_{18}ClNO_3$:** C, 65.16; H, 5.47; N, 4.22; Found: C, 65.09, H, 5.48; N, 4.23.

1-(2-(6-Bromonaphthalen-2-yl)-2-oxoethyl)piperidine-3-carboxylic acid (4S1e)

Yield: 222 mg, 59.3% as dark yellow oil. FT-IR (KBr, cm^{-1}): 3280 (OH Str.), 3073 (Ar-H Str.), 2979 (C-H Str.), 1712 (C=O Str.), 1380 (C-N Str.), 1265 (C-O Str.) 524 (C-Br Str.)**.** ^{1}H NMR (500 MHz, $CDCl_3$) δ ppm: 11.26 (s, 1H, COOH), 8.35 (s, 2H, naphthalene), 7.80 (s, 1H, naphthalene), 7.65 (d, *J* = 6.5 Hz, 1H, naphthalene), 7.61-7.58 (dd, *J* = 8.0 Hz, 2H, naphthalene), 3.60 (s, 1H, NCH_2), 3.50 (s, 1H, NCH_2), 2.70-2.30 (m, 5H, piperidine), 1.72-1.47 (m, 4H, piperidine). ^{13}C NMR (125 MHz, $CDCl_3$) δ ppm: 196.3, 174.0, 161.3, 138.1, 135.1, 133.1, 130.1, 129.8, 127.9, 126.8, 125.7, 123.6, 71.3, 63.1, 59.1, 47.3, 26.7, 21.3. Anal. calc. for **$C_{18}H_{18}BrNO_3$:** C, 57.46; H, 4.82; N, 3.72; Found: C, 57.60, H, 4.81; N, 3.52.

1-(2-(6,7-Dimethylnaphthalen-2-yl)-2-oxoethyl)piperidine-3-carboxylic acid (4S1f)

Yield: 188 mg, 57.7% as dark yellow oil. FT-IR (KBr, cm^{-1}): 3420 (OH Str.), 3102 (Ar-H Str.), 2962 (C-H Str.), 1725 (C=O Str.), 1391 (C-N Str.), 1198 (C-O Str.). ^{1}H NMR (500 MHz, $CDCl_3$) δ ppm: 11.80 (s, 1H, COOH), 8.20 (s, 1H, naphthalene), 8.00 (d, *J* = 7.5 Hz, 1H, naphthalene), 7.75 (d, *J* = 6.5 Hz, 1H, naphthalene), 7.55 (d, *J* = 8.0 Hz, 2H naphthalene), 3.60 (s, 1H, NCH_2), 3.50 (s, 1H, NCH_2), 2.80-2.30 (m, 5H, piperidine), 2.50 (s, 6H, naphthalene, 2×CH_3), 1.60-1.30 (m, 4H, piperidine). ^{13}C NMR (125 MHz, $CDCl_3$) δ ppm: 196.3, 174.0, 161.3, 138.3, 136.1, 133.1, 130.1, 129.8, 127.9, 126.8, 125.7, 123.6, 71.9, 58.5, 47.3, 25.6, 24.1, 22.5. Anal. calc. for **$C_{20}H_{23}NO_3$:** C, 73.82; H, 7.12; N, 4.30 Found: C, 73.91, H, 7.10; N, 4.29.

1-(2-(1-Methoxynaphthalen-2-yl)-2-oxoethyl)piperidine-3-carboxylic acid (4S1g)

Yield: 197 mg, 60.1% as dark yellow oil. FT-IR (KBr, cm^{-1}): 3345 (OH Str.), 3088(Ar-H Str.), 2897 (C-H Str.), 1698 (C=O Str.), 1367 (C-N Str.), 1254 (C-O Str.), 1051 (C-O Str.)**.** ^{1}H NMR (500 MHz, $CDCl_3$) δ ppm: 11.55 (s, 1H, COOH), 8.40 (d, *J* = 6.5 Hz, 1H, naphthalene), 8.10 (d, *J* = 7.5 Hz, 1H, naphthalene), 7.70-7.60 (m, 4H, naphthalene) 3.80 (s, 3H, naphthalene, OCH_3), 3.65 (s, 1H, NCH_2), 3.55 (s, 1H, NCH_2) 2.80-2.35 (m, 5H, piperidine), 1.65-1.40 (m, 4H, piperidine). ^{13}C NMR (125 MHz, $CDCl_3$) δ ppm: 196.3, 174.0, 161.3, 159.3, 138.3, 136.1, 133.1, 130.1, 129.8, 127.9, 126.8, 125.7, 123.6, 71.3, 57.1, 61.5, 47.3, 27.2, 21.4. Anal. calc. for **$C_{19}H_{21}NO_4$:** C, 69.71; H, 6.47; N, 4.28; Found: C, 69.52, H, 6.48; N, 4.28.

1-(2-(6,7-Dimethoxynaphthalen-2-yl)-2-oxoethyl)piperidine-3-carboxylic acid (4S1h)

Yield: 188 mg, 52.8% as dark yellow oil. FT-IR (KBr, cm^{-1}): 3266 (OH Str.), 2920(Ar-H Str.), 2754 (C-H Str.), 1691 (C=O Str.), 1405 (C-N Str.), 1215 (C-O Str.), 1048 (C-O Str.)**.** ^{1}H NMR (500 MHz, $CDCl_3$) δ ppm: 11.10 (s, 1H, COOH), 8.43 (s, 1H, naphthalene), 7.80 (d, *J* = 7.5 Hz, 1H, naphthalene), 7.50 (d, *J* = 8.5 Hz 2H naphthalene), 3.90 (s, 6H, naphthalene, 2×OCH_3), 3.68 (s, 1H, NCH_2), 3.59 (s, 1H, NCH_2), 2.70-2.30 (m, 5H, piperidine), 1.70-1.40 (m, 4H, piperidine). ^{13}C NMR (125 MHz, $CDCl_3$) δ ppm: 196.7, 177.0, 162.8, 158.3, 152.6, 151.3, 133.1, 130.1, 129.8, 127.9, 126.8, 125.7, 123.6, 71.3, 57.1, 56.5, 47.3, 25.9, 22.2. Anal. calc. for **$C_{20}H_{23}NO_5$:** C, 67.21; H, 6.49; N, 3.92; Found: C, 67.35, H, 6.50; N, 3.72.

1-(2-(6-Ethylnaphthalen-2-yl)-2-oxoethyl)piperidine-3-carboxylic acid (4S1i)

Yield: 191 mg, 58.9% as dark yellow oil. FT-IR (KBr, cm^{-1}): 3452 (OH Str.), 2978 (Ar-H Str.), 2735 (C-H Str.), 1710 (C=O Str.), 1425 (C-N Str.), 1087 (C-O Str.). ^{1}H NMR (500 MHz, $CDCl_3$) δ ppm: 10.50 (s, 1H, COOH), 7.98 (dd, *J* = 6.5 Hz, 1H, naphthalene), 7.67 (t, *J* = 1.5 Hz, 1H, naphthalene), 7.56 (d, *J* = 8.5 Hz, 1H,

naphthalene), 7.42-7.24 (m, 3H, naphthalene) 3.50 (s, 1H, NCH_2), 3.40 (s, 1H, NCH_2), 2.84-2.68 (m, 3H, piperidine), 2.66-2.41 (m, 2H, naphthalene, CH_2), 1.60-1.51 (m, 3H, piperidine), 1.23 (t, J = 6.5 Hz, 3H, naphthalene, CH_3). ^{13}C NMR (125 MHz, $CDCl_3$) δ ppm: 201.8, 181.2, 148.6, 142.9, 140.6, 136.1, 135.9, 133.5, 133.3, 132.2, 130.2, 68.8, 60.2, 58.4, 45.8, 33.2, 29.7, 27.4, 18.0. Anal. calc. for **$C_{20}H_{23}NO_3$:** C, 73.82; H, 7.12; N, 4.30; Found: C, 73.69, H, 7.11; N, 4.29.

5.A.2. BIOLOGICAL ACTIVITY

5.A.2.1. *In Vivo* Anti-convulsant Activity

5.A.2.1.1. s.c.-PTZ Induced Seizures in Mice

The role of the GABAergic system in the genesis of epilepsy is well documented and understood. The imbalance in the inhibitory and excitatory pathways is triggered by chemical or electrical impulses leading to the generation of seizures. As a consequence, any drug supporting the inhibitory function of GABA directly or indirectly has the potential to suppress epilepsy and associated phenomena. Tiagabine, a derivative of nipecotic acid is one of these kinds of drug. Tiagabine reduces neuronal excitability by inhibiting GABA uptake into glia and neurons [Nielsen *et al*., 1991]. It increases synaptosomal concentrations of the inhibitory neurotransmitter GABA via inhibition of the GABA transporter GAT-1 [Bauer and Cooper-Mahkorn, 2008].

In this test, rodents were challenged a subcutaneous dose of PTZ, one hour after the administration of test compounds and the standard drug and were observed for 30 minutes. It has been reported that a subcutaneously injected convulsive dose of PTZ induces a clonic seizure of at least 5 s duration in 97% of the animals (CD97) [Löscher, 2011]. PTZ causes convulsions by interacting with picrotoxin binding cite at $GABA_A$ receptor complex [De Deyn *et al*., 1992]. Compounds **3S1a, 3S1b, 3S1i, 4S1a, 4S1b,** and **4S1i** exhibited a significant delay in the onset of convulsion similar

to tiagabine in comparison to control group **(Table 5.2.)**. The further inter-group comparison revealed that the antiepileptic potential of derivatives **4S1a, 4S1b** and **4S1i** were superior to that of **3S1a, 3S1b,** and **3S1i**. Substitution at the **R6** position of the acetonaphthone ring with an election withdrawing substituent diminished the antiepileptic activity that was observed in compounds **3S1c, 3S1d, 3S1e** and **4S1c, 4S1d, 4S1e**. Also, substitution of hydrogen with any other group at the R7 position also affected the antiepileptic effect (**3S1f** and **4S1f**).

Table 5.2. Effect of test compounds (**Series-1**) on *s.c.*-PTZ induced seizures

Comp.	Latency of seizures (seconds)*	Frequency of seizures (numbers)*
Control	627.66 ± 37.97	3.83 ± 0.75
3S1a	731.50 ± 45.71[a]	1.83 ± 0.75[a]
3S1b	728.66 ± 37.81[a]	1.83 ± 0.40[a]
3S1c	647.33 ± 34.12	3.33 ± 1.03
3S1d	614.83 ± 62.05	3.66 ± 0.83
3S1e	638.50 ± 35.20	3.00 ± 0.63
3S1f	624.16 ± 18.83	3.50 ± 0.83
3S1g	646.16 ± 43.83	3.16 ± 0.75
3S1h	655.16 ± 34.42	3.66 ± 0.81
3S1i	735.83 ± 26.79[a]	2.16 ± 0.96
4S1a	1079.16 ± 36.41[a,b]	1.16 ± 0.40[a,b]
4S1b	1138.16 ± 38.55[a,b]	1.00 ± 0.00[a,b]
4S1c	640.33 ± 57.19	3.00 ± 1.09
4S1d	653.50 ± 51.55	3.16 ± 1.16
4S1e	644.33 ± 34.54	3.16 ± 0.40
4S1f	626.66 ± 59.30	3.33 ± 1.03
4S1g	663.66 ± 25.04	2.83 ± 1.16
4S1h	654.33 ± 41.14	2.66 ± 0.51
4S1i	1226.33 ± 69.53[a,b]	1.00 ± 0.63[a,b]
Tiagabine	1331.83 ± 41.16[a]	1.00 ± 0.00[a]

* Values are expressed as the Mean ± SD (n = 6); Control: Physiological saline (0.9%) containing 2.5% tween 80; Tiagabine: 10mg/kg/i.p.;All the test compounds were administered intraperitoneally at an equimolar dose relative to 10mg/kg tiagabine; a $p < 0.05$ compared to Control; b $p < 0.05$ compared to compounds 3S1a, 3S1b, and 3S1i.

Based on the outcome of this study, the antiepileptic activity of the derivatives (**3S1a, 3S1b, 3S1i 4S1a, 4S1b**, and **4S1i**) may be attributed to their ability to increase the level of GABA in a manner similar to tiagabine.

5.A.2.1.2. Pilocarpine-induced seizures in mice

Pilocarpine induced seizures is a rodent model of status epilepticus used to assess the antiepileptic activity of NCE's towards seizures originating from the temporal lobe [Curia *et al*., 2008]. Pre-treatment with test compounds delayed the onset of seizures, status epilepticus, and death. Compounds **4S1a, 4S1b,** and **4S1i** along-with tiagabine exhibited a statistically significant protection against pilocarpine-induced seizures whereas their ester counterpart **3S1a, 3S1b,** and **3S1i** were comparatively less effective in delaying the onset of seizures **(Table 5.3.)**.

Table 5.3. Effect of test compounds (**Series 1**) on pilocarpine-induced seizures

Comp.	Latency of seizures (seconds)*	Latency to death (seconds)*
Control	313.83 ± 27.30	447.83 ± 31.56
3S1a	348.16 ± 10.34[a]	516.16 ± 39.59[a]
3S1b	347.83 ± 10.75[a]	513.50 ± 18.93[a]
3S1i	352.16 ± 12.98[a]	521.50 ± 26.49[a]
4S1a	437.50 ± 21.40[a,b]	583.50 ± 23.51[a,b]
4S1b	460.16 ± 11.82[a,b]	654.16 ± 22.87[a,b]
4S1i	531.16 ± 20.87[a,b]	767.83 ± 53.51[a,b]
Tiagabine	564.16 ± 18.01[a]	838.16 ± 36.51[a]

[*] Values are expressed as the Mean ± SD (n = 6); Control: Physiological saline (0.9%) containing 2.5% tween 80; Tiagabine: 10mg/kg/*i.p.;*All the test compounds were administered intraperitoneally at an equimolar dose relative to 10mg/kg tiagabine; [a] $p < 0.05$ compared to Control; [b] $p < 0.05$ compared to compounds **3S1a, 3S1b,** and **3S1i.**

Tiagabine has been reported in effectively protecting rodents against pilocarpine-induced convulsions [Sałat *et al*., 2015]. Also, in a recent study by Sałat *et al*., it was reported that DDPM-2571, a GAT-1 inhibitor was highly effective in the prevention of chemically-induced seizures both by pentylenetetrazole and Pilocarpine

[Sałat *et al*., 2017]. Thus it is evident that compounds which increase the concentration of GABA at the synaptic cleft are promising candidates as potential antiepileptic agents.

5.A.2.1.3. DMCM induced seizures in mice

DMCM belongs to the beta-carboline group of compounds and acts as a negative allosteric modulator at the benzodiazepine-binding site on the $GABA_A$ receptor. Besides attenuation of GABA-mediated inhibition, augmentation of excitatory amino acid by DMCM has been suggested as a mechanism of inducing epilepsy. Kulick *et al*., have demonstrated that tiagabine protected against DMCM-evoked seizures in rats [Kulick *et al*., 2014]. The outcome of the DMCM induced seizures in mice illustrates that compounds **4S1a, 4S1b, 4S1i,** and **tiagabine** exhibited a significant delay in onset of seizures induced by DMCM in comparison to control **(Table 5.4.)**. Once again, compounds **3S1a**, **3S1b**, and **3S1i** were comparatively less effective in protecting against seizures in this test. It was observed that compound **4S1i** is statistically comparable to tiagabine in this model.

Table 5.4. Effect of test compounds (**Series 1**) on DMCM induced seizures

Comp.	Latency of seizures (seconds)*
Control	230.83 ± 13.83
3S1a	272.16 ± 11.58[a]
3S1b	278.66 ± 22.21[a]
3S1i	282.66 ± 17.75[a]
4S1a	352.16 ± 28.63[a,b]
4S1b	402.33 ± 14.27 [a,b]
4S1i	454.83 ± 21.64 [a,b]
Tiagabine	466.16 ± 14.71[a,b]

[*] Values are expressed as the Mean ± SD (n = 6); Control: Physiological saline (0.9%) containing 2.5% tween 80; Tiagabine: 10mg/kg/*i.p.*;All the test compounds were administered intraperitoneally at an equimolar dose relative to 10mg/kg tiagabine; [a] $p < 0.05$ compared to Control; [b] $p < 0.05$ compared to compounds **3S1a, 3S1b,** and **3S1i.**

5.A.2.2. Rota-rod Performance Test in Mice

The rota-rod test is widely used to evaluate the effect of compounds on the motor coordination of rodents [Shiotsuki *et al*., 2010]. In this experiment, hybrids **4S1a, 4S1b, 4S1i** and tiagabine did not cause any alteration in "fall-off" time on rotating rods as compared to control indicating their inability to induce any observable signs of impairment in muscle co-ordination thereby affecting the motor performance and skeletal, muscular strength of the treated animals **(Table 5.5)**. Standard drug diazepam was however seen to significantly reduce the "fall-off" time post-treatment.

Table 5.5. Effect of test compounds (**Series 1**) on rota-rod performance test in mice

Comp.	Fall off time before treatment (seconds)*	Fall off time after treatment (seconds)*
Control	334.16 ± 29.78	336.16 ± 28.84
4S1a	321.16 ± 11.99	323.33 ± 12.38
4S1b	332.16 ± 13.37	334.83 ± 13.65
4S1i	321.50 ± 11.74	325.83 ± 11.89
Tiagabine	335.83 ± 11.44	339.16 ± 11.08
Diazepam	325.83 ± 9.47	181.66 ± 25.47[a]

[*] Values are expressed as the Mean ± SD (n = 6); Control: Physiological saline (0.9%) containing 2.5% tween 80; Tiagabine: 10mg/kg/*i.p.;* Diazepam: 4mg/kg.*i.p.*; All the test compounds were administered intraperitoneally at an equimolar dose relative to 10mg/kg tiagabine; [a] $p < 0.05$ compared to Control.

5.A.2.3. Cell viability and neurotoxicity (MTT Assay)

Some antiepileptic drugs and their metabolites have been reported to possess neurotoxicity [Ambrósio *et al*., 2000; Araújo *et al*., 2004; Gao and Chuang, 1992; Gao *et al*., 1995; Liu *et al*., 2015; Nonaka *et al*., 1998]. Ideally, antiepileptic drugs should prevent the seizures without producing neuronal toxicity. Therefore, the therapeutic suitability of the most active compounds **(4S1a, 4S1b, & 4S1i)** and their effects on cell viability was determined in neuroblastoma cell line (SH-SY5Y). The

ability of intracellular dehydrogenases to reduce MTT to the formazan, is interpreted as the measure of cell viability **(Fig 5.1)**.

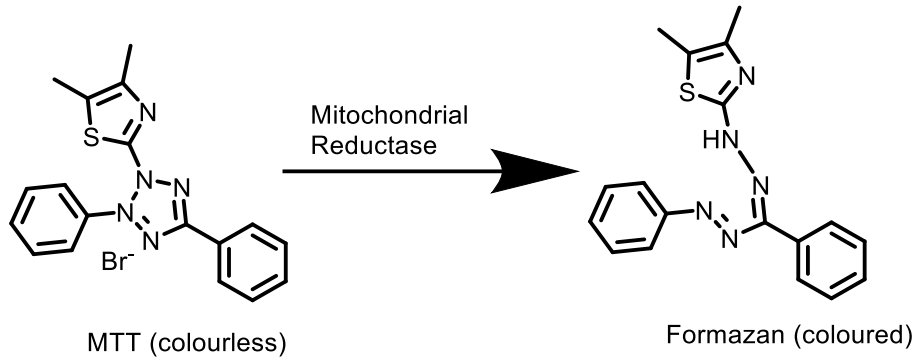

Fig. 5.1 Conversion of MTT to formazan in the presence of mitochondrial dehydrogenase

The formazan upon solubilization can be measured spectrophotometrically, which is directly proportional to the viable cell number [Lim *et al*., 2015]. The results of the experiment reveal that the MTT reduction was not effected significantly by test compounds **(4S1a, 4S1b, & 4S1i)**, thus corresponds to the insignificant cell death in the concentrations of the test compounds ranging from 1µM to 80 µM **(Table 5.6.)**.

Table 5.6. Percentage cell viability of the test compounds (**Series 1**) at different concentrations in neuroblastoma cell line (SH-SY5Y).

Comp.	Percentage cell viability*				
	1 µm	**10 µm**	**20 µm**	**40 µm**	**80 µm**
4S1a	99.59 ± 0.04	99.79 ± 0.10	99.79± 0.12	98.21 ± 0.17	91.36 ± 0.13
4S1b	99.44 ± 0.06	99.36 ± 0.11	98.39 ± 0.27	96.37 ± 0.15	90.95 ± 0.21
4S1i	99.71 ± 0.08	99.61 ± 0.07	98.47 ± 0.23	95.91 ± 0.31	91.09 ± 0.19

* Percentage cell viability of SH-SY5Y cells incubated with increasing concentration of test compounds. Values are expressed as the percentage cell viability ± SD of at least five independent experiments.

5.A.2.4. Repeated dose toxicity studies

Owing to the reported haematological, renal and hepatic side effects of antiepileptic drugs [Tolou-Ghamari *et al*., 2013; Bachmann *et al*., 2011; Hamed, 2017; Gram and

Bentsen, 1983], the assessment of the related parameters is of paramount necessity. The body weights of test compound **(4S1i)** treated group were normal in comparison to the control group. As compared to the control group, daily food and water intakes were also not significantly changed in test compound **(4S1i)** treated groups. Compound **4S1i** showed no significant change in the levels of haemoglobin, TLC, and DLC. It is apparent from observed data that the serum levels of glucose, cholesterol, alkaline phosphatase, AST, ALT, blood urea nitrogen, creatinine and total protein were also not altered significantly in the group treated with compound **4S1i**. The results of haematological and biochemical parameters are summarized in table **Table 5.7** and **Table 5.8** respectively. The outcome of the estimation of various haematological and biochemical parameters confirms the safety of the compound **4S1i** at an equimolar dose relative to 10 mg/kg tiagabine.

Table 5.7. Effect of test compound **(4S1i)** on hematological parameters of mice in 28 days repeated dose toxicity studies

Treatment	Hemoglobin (gm/dl)	Total WBC (X 10^3/µl)	Differential Leukocytes Count (%)				
			Neutrophil	Lymphocyte	Eiosinophil	Monocyte	Basophil
Control	11.71 ± 0.59	5.48 ± 0.49	64.06 ± 2.66	33.38 ± 2.57	1.66 ± 0.30	0.88 ± 0.30	00
4S1i	11.90 ± 0.95	5.26 ± 0.26	64.14 ± 3.35	33.16 ± 3.26	1.86 ± 0.55	0.80 ± 0.20	00
Tiagabine	12.35 ± 0.64	5.58 ± 037	63.75 ± 2.94	33.74 ± 2.75	1.72 ± 0.26	0.78 ± 0.02	00

Values are mean ± SD (n=6), WBC= White blood corpuscles.

Table 5.8. Effect of test compound **(4S1i)** on biochemical parameters of mice in 28 days repeated dose toxicity studies

Treatment	Glucose (mg/dl)	Cholesterol (mg/dl)	AST (U/ml)	ALT (U/ml)	ALP (Unit)	Blood Urea (mg/dl)	Creatinine (mg/dl)	Total Protein (gm/dl)
Control	89.50 ± 3.61	105.55 ± 7.55	42.83 ± 3.43	39.33 ± 2.94	240.83 ± 2.94	12.24 ± 1.27	0.86 ± 0.07	5.15 ± 0.20
4S1i	87.16 ± 2.63	103.33 ± 6.05	41.66 ± 2.94	38.83 ± 3.18	239.50 ± 9.24	13.31 ± 1.75	0.82 ± 0.09	4.93 ± 0.35
Tiagabine	90.16 ± 6.06	100.66 ± 7.00	40.33 ± 4.03	37.50 ± 1.76	243.50 ± 5.31	12.28 ± 1.88	0.85 ± 0.07	5.06 ± 0.31

Values are mean ± SD (n=6), AST= Aspartate transaminase, ALT= Alanine transaminase, ALP= Alkaline phosphatase.

5.A.2.5. *In Vitro* Parallel Artificial Membrane BBB Permeability (PAMPA-BBB) Assay

The main impediment for nipecotic acid is to cross the highly selective BBB and to reach the target site. Therefore, lipophilic analogs were synthesized, in order to facilitate their permeation across BBB. To precisely predict the transport of the synthesized derivatives through the BBB, the permeability of the lead compounds **4S1a, 4S1b,** and **4S1i** was assessed by the parallel artificial membrane permeation assay (PAMPA-BBB) as per the reported procedure. The validation of the assay was performed by comparing the experimentally determined permeability of nine commercially available drugs with that of the values reported in the literature. A plot of experimentally obtained permeability [$P_{e(exp)}$] versus permeability reported in the literature [Pe(ref)] provided a good linear correlation $P_{e(exp)} = 1.308\ P_{e(ref)} - 0.8394$ (R^2=0.9317). Using this equation, the cut-off limits were calculated for the determination of BBB permeability of the test compounds. The values of $P_{e(ref)}$ has been taken from the limits established by Di *et al.* [Di *et al*., 2003].

The findings suggest that the evaluated derivatives exhibited considerable permeability to cross BBB (**Table 5.9**). Also, the permeability (P_e) of the lead derivative **4S1i** in the assay was found to be **8.89** which reveal that it is comparatively more permeable than standard drug Tiagabine, the *Pe* of which was found to be **7.86**. Also, the outcome indicates that **4S1i** is relatively more permeable than **4S1a** and **4S1b**.

Table 5.9. PAMPA- BBB permeability (P_e) value for commercial drugs, Tiagabine (Standard), selected leads of **Series 1**.

Comp.	PAMPA- BBB permeability[a] $P_{e(exp)}$ (10^{-6} cm s^{-1})	PAMPA- BBB Prediction (CNS+[b], CNS-[c], CNS±[d])
Validation of the model by nine commercial drugs		
Verapamil	16.00	CNS+
Diazepam	16.00	CNS+
Progesterone	9.30	CNS+
Atenolol	0.80	CNS-
Dopamine	0.20	CNS-
Lomefloxacin	1.10	CNS-
Alprazolam	5.40	CNS+
Chlorpromazine	6.50	CNS+
Oxazepam	10.00	CNS+
Evaluation of P_e (10^{-6} cm s^{-1}) for the test compounds and standard		
Tiagabine (standard)	7.86	CNS+
4S1a	5.84	CNS+
4S1b	7.24	CNS+
4S1i	8.89	CNS+

[a]Data represented are the mean of assay for commercial drugs (n = 2);
[b]'CNS+' (prediction of high BBB permeation); P_e (10^{-6} cm s^{-1}) > 4.3926.
[c]'CNS-' (prediction of low BBB permeation); P_e (10^{-6} cm s^{-1}) < 1.7766.
[d]'CNS±' (prediction of uncertain BBB permeation); P_e (10^{-6} cm s^{-1}) 4.3926 to 1.7766

5.A.3. COMPUTATIONAL STUDIES

5.A.3.1. Homology modeling of GAT-1

Construction of a 3D model of the protein is possible through homology modeling. Homology modeling principally involves three steps including (a) alignment of the amino acid sequence of selected Template (b) model preparation, followed by (c) validation. Human GAT1 protein has been selected for model building. Drosophila dopamine transporter (dDAT), is one of the closest transporter

protein related to human GAT1 for which structures are available. Using dDAT structure as template homology model of both the occluded and the open-to-out conformations were created. After the alignment, 46% sequence identity and 67% similarity of the 4XP4 template with GAT1 sequence has been obtained **(Fig. 5.2)**.

The models were exhaustively tested and verified through comparison to functional and mutational data reported in the literature. The homology model was evaluated through computations of molecular interactions fields and sequence identities. In Ramachandran plot, all the residues except Phe174 and Ser178 were present in the allowed region **(Fig. 5.3)**. The putative spots for the ligand selectivity were then identified. Template in an open-to-out conformation was used for allowing access to bulky synthesized molecules. A validated homology model was obtained followed by the identification of putative spots for ligand (Tiagabine) selectivity. Tiagabine was added as a co-crystallized ligand in the model which was further utilized for molecular docking and dynamics.

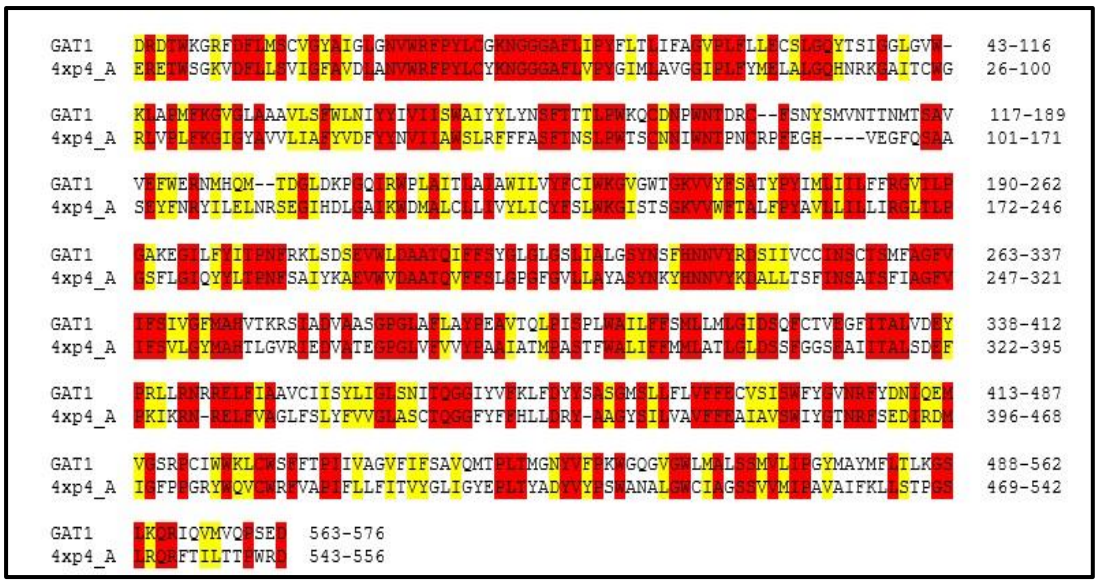

Fig. 5.2. Sequence alignment between GAT1 and drosophila melanogaster dopamine transporter. Identical residues are colored in red, while similar residues are colored in yellow.

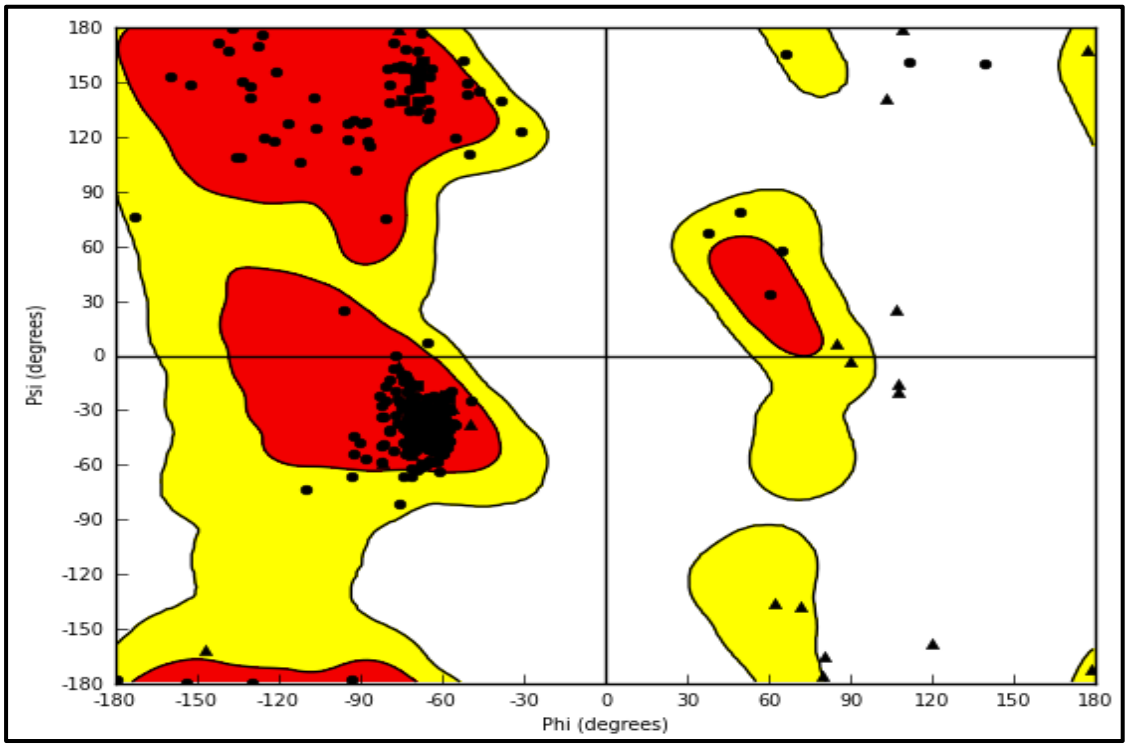

Fig. 5.3. Ramachandran plot of the GAT1. 3-dimensional model showing the dihedral angles of the amino acids

5.A.3.2. Molecular Docking Studies

In silico docking studies were performed using the Schrödinger Maestro program to gain insight into the possible mode of protein-ligand interactions using a generated and validated model of GAT1 GABA transporter. The validation of the prepared grid and docking protocols was performed by generating a minimum energy conformer of tiagabine, and it's docking on a prepared grid. The results demonstrate that tiagabine occupied the same active site within the binding pocket leading to its consensual interaction with the amino acid residues within the active site **(Fig. 5.4)** [Jurik *et al*., 2015; Petrera *et al*., 2016; Skovstrup *et al*., 2010].

The potential hybrids **4S1a, 4S1b,** and **4S1i** based on the outcome of *in vivo* pharmacological evaluations were selected for *in silico* docking studies. The results of docking simulations reveal that compounds **4S1a** (GLIDE Score: -5.8); **4S1b** (GLIDE Score: -4.9) and **4S1i** (GLIDE Score: -7.3) have occupied the active binding pocket leading to their interaction with active site residues similar to tiagabine **(Fig. 5.5, Fig. 5.6 & Fig. 5.7)**.

The inspection of docked poses of compound **4S1a, 4S1b,** and **4S1i** showed that the O atom of carboxyl group interacted with Na611 through a salt bridge formation. Another O atom present in carboxyl group of compound **4S1i** shown to have additional metal coordination interaction with Na611. The O atom of the carboxyl group in all the potential hybrids also interacted through a network of hydrogen bonding with backbone atoms of Gly65 and the side chain hydroxyl groups of Tyr140. Additionally, the phenyl ring of compound **4S1b** was also stabilized through π- π stacking interaction with Phe294. The carbonyl side chain of compound

4S1i was involved in hydrogen bonding interaction with a side chain amino group of Gln291. The charged interactions with Arg69 and Asp451 were also responsible for stabilizing the aromatic rings of compound **4S1i**. The detailed interaction results of tiagabine, **4S1a, 4S1b,** and **4S1i** with active site amino acid residues are summarized in **Table 5.10.** Overall, these interactions of all the docked ligands with the modelled protein of GAT1 GABA transporter showed consensual binding with active site amino acids residues leading to its effective inhibition.

Table 5.10. Details of protein-ligand interactions of **tiagabine, 4S1a, 4S1b, and 4S1i**

Comp.	Parameters					
	Glide Score	Interacting residues*				
		Hydrogen bonding	Salt bridge	pi-pi stacking	Metal coordination bond	Other Interacting residues
Tiagabine	-4.6	Gly65, Tyr140, Phe294	Na611	None	None	Tyr60, Ala61, Gly63, Trp68, Arg69, Tyr139, Ile143, Gln291, Ser295, Gly297, Phe447, Asp451
4S1a	-5.8	Gly65, Tyr140	Na611	None	None	Tyr60, Gly63, Tyr139, Phe294, Gly297, Leu300, Ser396, Asp451, Ala455, Ser456, Leu460
4S1b	-4.9	Gly65, Tyr140	Na611	Phe294	None	Gly63, Leu64, Arg69, Thr290, Gln291, Ser295, Tyr452
4S1i	-7.3	Gly65, Tyr140, Gln291	Na611	None	Na611	Gly63, Leu64, Arg69, Phe294, Ser295, Tyr452, Gly457

* All the interactions were observed within 4Å distance.

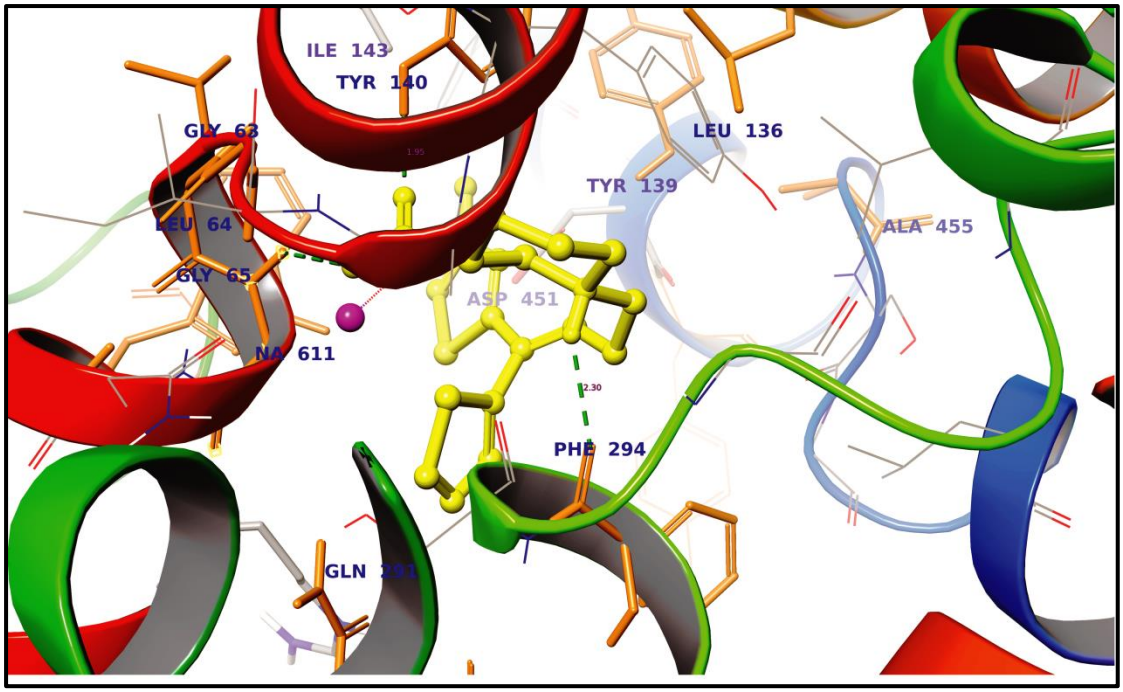

Fig. 5.4. Docked pose of the tiagabine on homology modeled protein structure of GAT1 GABA transporter. Ribbon representation of protein showing active site binding interaction of tiagabine (ball & stick model)

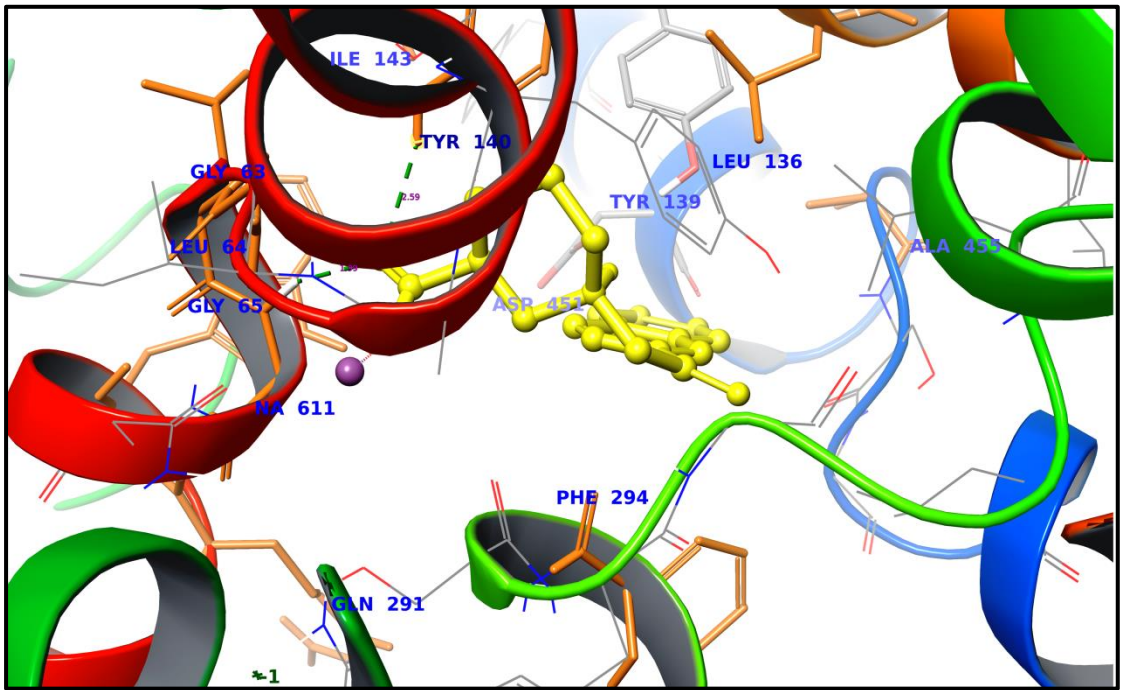

Fig. 5.5. Docked pose of the **4S1a** on modeled protein structure of GAT1 GABA transporter. Ribbon representation of protein showing active site binding interaction of **4S1a** (ball & stick model).

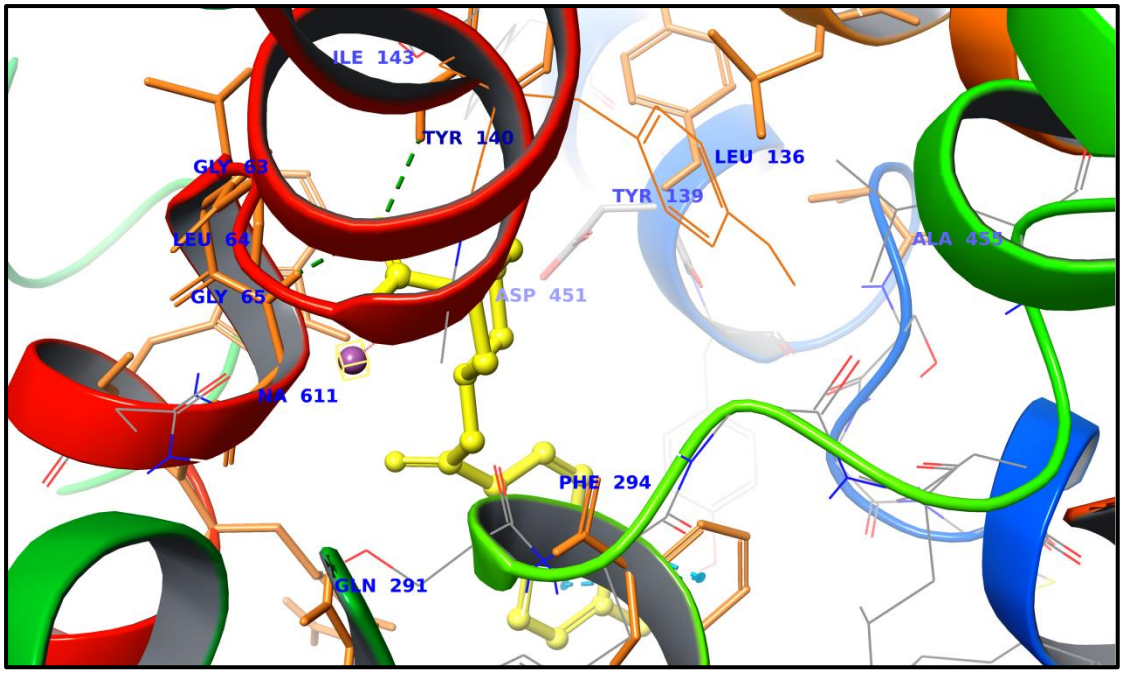

Fig. 5.6. Docked pose of the **4S1b** on modeled protein structure of GAT1 GABA transporter. Ribbon representation of protein showing active site binding interaction of **4S1b** (ball & stick model).

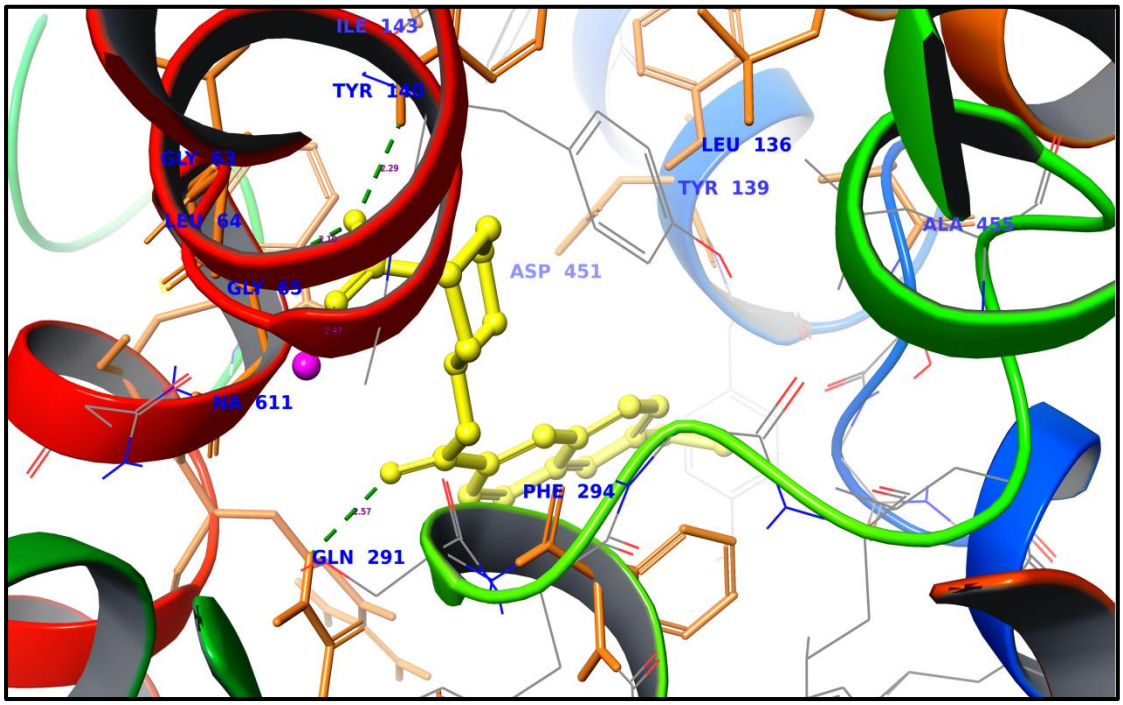

Fig. 5.7. Docked pose of the **4S1i** on modeled protein structure of GAT1 GABA transporter. Ribbon representation of protein showing active site binding interaction of **4S1i** (ball & stick model).

5.A.3.3. Molecular Dynamics

The dynamics simulation runs of the generated minimized complex of **4S1i** with GABA GAT1 transporter protein of 4XP4 was performed for 20 ns to predict the stability of binding mode interactions. The overall stability of the system was evaluated by RMSD (Root Mean Square Deviation) and RMSF (Root Mean Square Fluctuation) calculations. The results of the RMSD values confirmed that all frames of the complex were in trajectory throughout the simulation with average fluctuation in the range of 0.4 Å **(Fig. 5.8)**.

The structural stability of the protein and ligand **4S1i** was further confirmed by calculating protein and ligand RMSF, respectively. The RMSF value obtained below 3 Å confirmed the absence of overall local changes along the protein chain and ligand atom position along the complete phase of the dynamic simulation run **(Fig. 5.9)**.

The graphical representation of binding interactions of compound **4S1i** showed the active site interactions throughout the simulation run **(Fig. 5.10)**. The results demonstrated that compound **4S1i** efficiently interacted with active site residues Leu64, Gly65, and Tyr140 through H-bonds. Besides, it also interacted with Phe294 through hydrophobic interactions.

The interaction fraction with individual amino acid residues was also calculated and represented in a stacked bar chart **(Fig. 5.11)**. The interaction fraction of a percentage of total contact maintained throughout the run. For example, 0.6 suggests that interaction was maintained 60% of the total simulation run.

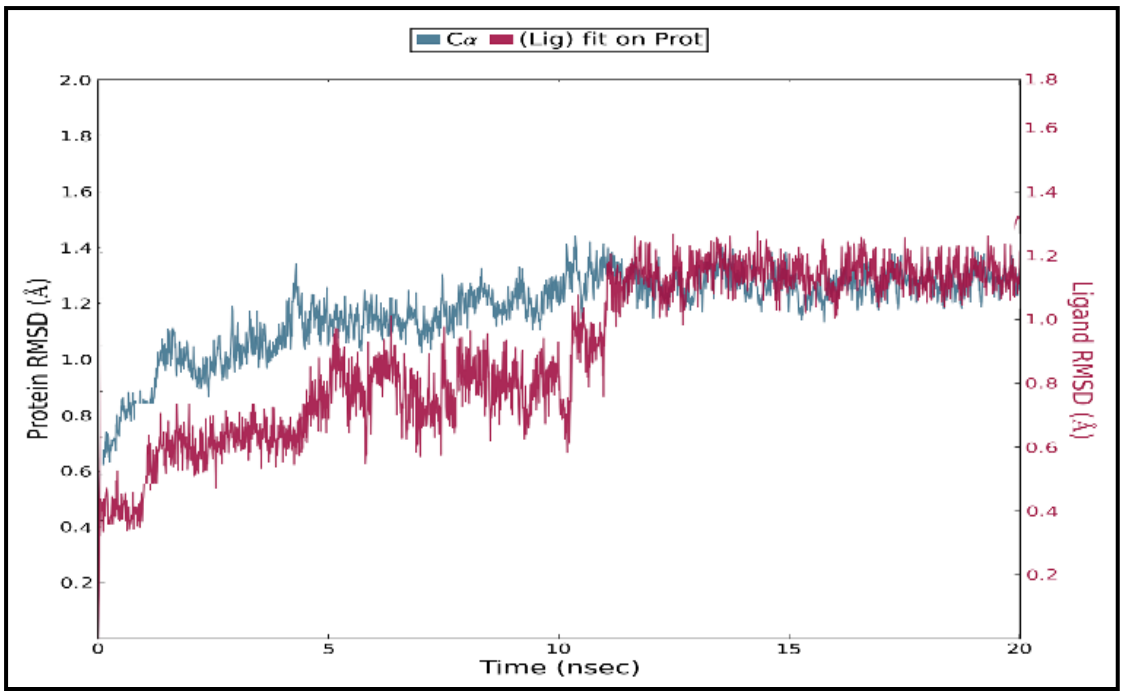

Fig. 5.8. Protein RMSD (Left Y-Axis) and ligand RMSD (Right Y-Axis) values in Å with time in ns (X-Axis).

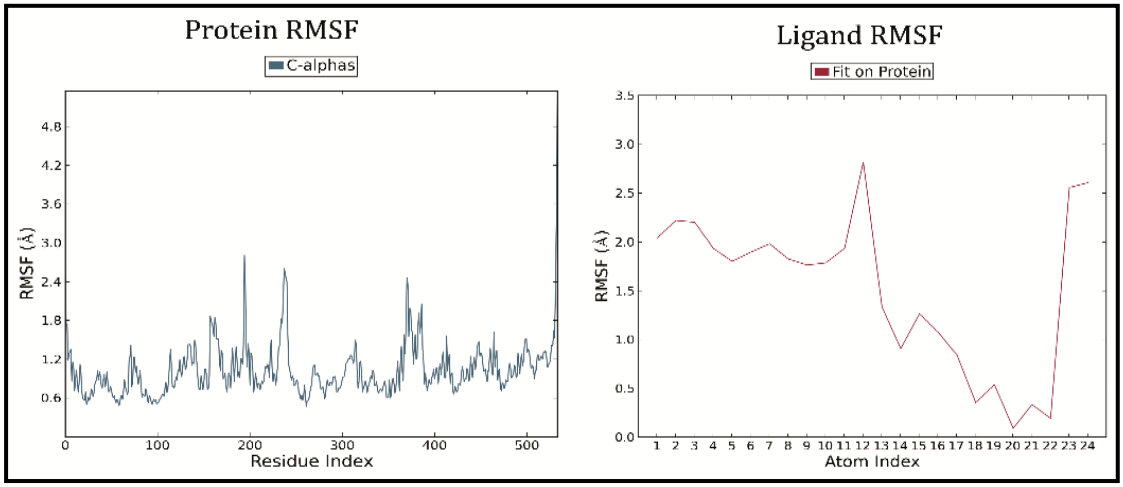

Fig. 5.9. Protein RMSF (Left side) and ligand RMSF (Right side) values in Å with time in ns.

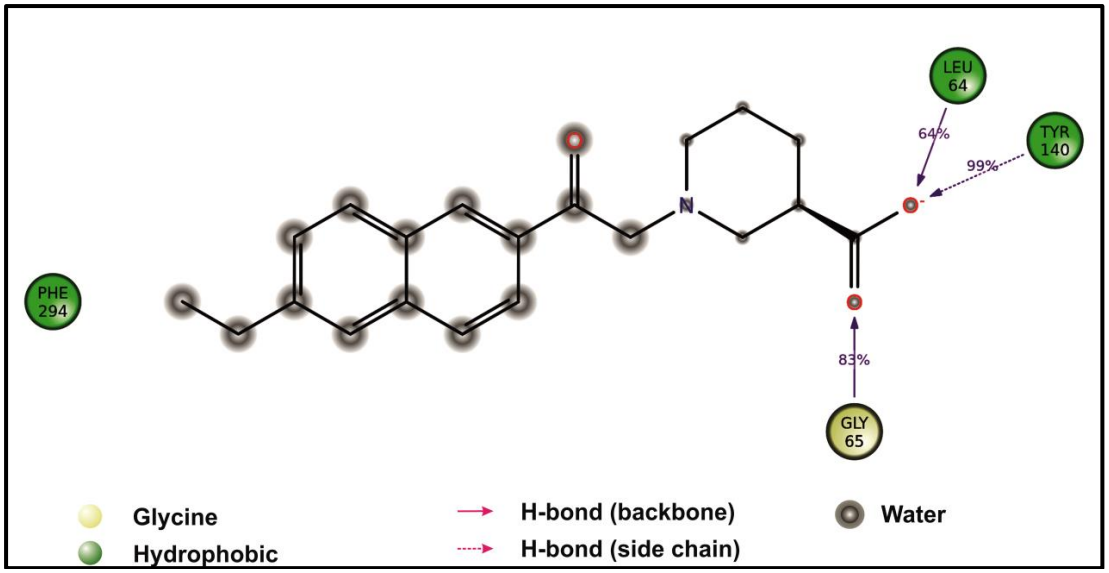

Fig. 5.10. The detailed atomic interactions of ligand **4S1i** with the key active amino acid residues.

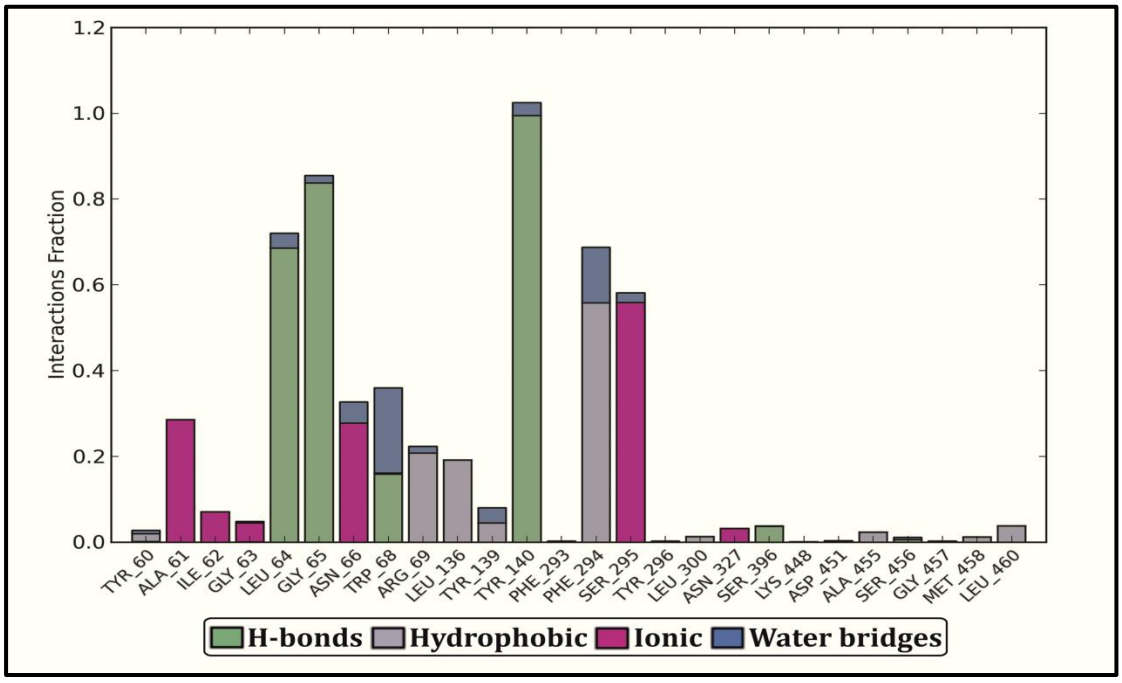

Fig. 5.11. Stacked bar charts of protein interactions with ligand 4S1i as monitored throughout the MD simulation.

5.A.3.4. Estimation of "Drug-Like" Properties

By using QikProp module of Schrödinger Maestro 10.5.014 in silico, "drug likeliness" of the most active derivatives **(4S1a, 4S1b & 4S1i)** has been predicted. The estimated results of some key parameters are mentioned in **Table 5.11**. Lipophilicity is the key requisite for the synthesized compounds for CNS activity. Predicted values for **QPlogBB** and **CNS** activity indicate that the selected compounds were active for CNS and may cross the BBB [Ugale and Bari, 2016]. The predicted log P values were also found within the range, but the experimental values differ with that of the predicted ones. Usually, the compounds designed for CNS disorders should have a lower polar surface area **(PSA)** [Zerroug et al. 2018]. To get entry in the brain, an upper limit of 90 has been reported for **PSA** [Pajouhesh and Lenz, 2005]. The predicted **PSA** values were found to be in the range of 79.014-79.015, which revealed that the selected compounds exhibit lower polar surface area and may have the ability to cross BBB.

The predicted "**rtvFG**" (Number of reactive functional groups) value was found to be 0 for all the tested compounds, which suggests the absence of reactive functional groups that cause decomposition, reactivity, or toxicity problems *in vivo*. The compounds exhibited drug likeliness based on Lipinski's rule of five (**mol_MW** < 500, **QPlogPo/w** < 5, **donorHB** 6≤ 5, **accptHB** ≤10). **QPlogKHSA** values for the tested compounds fall within the limit [Lipinski et al. 2012], indicating considerable binding of the compounds with plasma proteins. Overall the predicted parameters revealed that the compounds **4S1a, 4S1b,** and **4S1i** fulfil drug-like characteristics.

Table 5.11. *In silico* drug likeliness properties of active compounds of **Series 1**

Comp.	Mol_MW (130-725)	PSA (7-200)	QPlogBB (-3-1.2)	QPlog Po/w (-2-6.8)	CNS (-2-+2)	#rtvFG (0-2)	Lipinski's rule of five (Max. 4)	QPlogKHSA	donorHB (0-6)	accptHB (2-20)
4S1a	297.353	79.014	-0.568	0.493	0	0	0	-0.173	1	6
4S1b	311.38	79.015	-0.608	0.794	0	0	0	-0.023	1	6
4S1i	325.407	78.044	-0.656	1.181	0	0	0	0.09	1	6

Mol_MW: molecular weight;
PSA: polar surface area;
QPlogBB: Predicted brain/blood partition coefficient;
QPlogPo/w: Predicted octanol/water partition coefficient;
CNS: Predicted central nervous system activity;
#rtvFG: Number of reactive functional group;
Rule of five: No. of violations of Lipinski's rule of five;
QPlogKHSA: Prediction of binding to human serum albumin;
donorHB: No. of hydrogen bonds that would be donated by the solute to water molecules in an aqueous solution;
accptHB: No. of hydrogen bonds that would be accepted by the solute from water molecules in an aqueous solution.